AN OCCURRENCE OF METASOMATIC ALUMINOSILICATES RELATED TO HIGH ALUMINA HYDROTHERMAL ALTERATION WITHIN THE SOUTH MOUNTAIN BATHOLITH, NOVA SCOTIA

Michael C. Corey
Nova Scotia Department of Mines and Energy
Halifax, Nova Scotia B3J 2X1

A zone of high alumina hydrothermal alteration (HAHA) is documented within granitoid rocks of the Big Indian Polyphase Intrusive suite (BIPI suite), which forms part of the Late Devonian-Early Carboniferous South Mountain Batholith (SMB). The alteration, which is confined to a NE-trending shear zone, is characterized by the quartz-deficient mineral assemblage andalusite-sillimanite-spinel-muscovite-cordierite-apatite-pyrite. The HAHA zone represents the first reported occurrence of this alteration type within the South Mountain Batholith.

Field observations indicate that the HAHA zone is only one of a series of successive and superimposed metasomatic-hydrothermal events which, together with W-Cu-Mo + U-Cu mineralization, exhibit a transition in style from early pervasive to late fracture-controlled. This change in style within the BIPI suite is considered to reflect a progressive increase in fluid pressure.

Petrography and mineral chemistry suggest that the HAHA zone formed in response to the interaction of the leuco-monzogranite host with a Na($\pm$Al)-rich, silica-undersaturated fluid. Although speculative, alumina may have been a mobile element transported as an alkali-complex via the fluid. High temperature mineral assemblages (andalusite-sillimanite; andalusite-spinel) indicate that the initial temperature of the aqueous fluid phase was $\geq 620^\circ$C for 2 kb pressure. It is proposed that the fluid phase represents a residual magmatic-fluid which was accessed by deep-seated fracturing.

On documente une zone d'altération hydrothermale hautement alumineuse (AHHA) à l'intérieur des granitoïdes de la suite Intrusive Polyphasée de Big Indian (suite IPBI) qui fait partie du Batholite de South Mountain (BSM) d'âge tardidévonien à éocarbonifère. Confinée à une zone de cisaillement à tendance NE, l'altération est caractérisée par un assemblage de minéraux, déficient en quartz, à andalousite-sillimanite-spinelle-muscovite-cordiérite-apatite-pyrite. La zone AHHA représente la première mention de ce type d'altération à l'intérieur du BSM.

D'après les observations sur le terrain, cette zone AHHA n'est qu'un d'une série d'événements métasomatiques et hydrothermaux successifs et superposés qui, ainsi qu'une minéralisation en W-Cu-Mo+U-Cu, exhibent un style d'abord pénétrant et enfin filonien. On considère que ce changement de style à l'intérieur de la suite IPBI représente un accroissement progressif de la pression des fluides.

La pétrographie et le chimisme des minéraux tendent à montrer que la zone AHHA s'est établie en réponse à l'intéraction de l'encaissant leucomonzogranitique avec un fluide sous-saturé en silice et riche en Na($\pm$Al. Bien que cela reste spéculatif, l'alumine pourrait avoir été un élément mobile transporté par le fluide à l'état de complexe alcalin. D'après les assemblages de minéraux à haute température (andalousite-sillimanite; andalousite-spinelle), la température initiale de la phase aqueuse fluide était >620°C pour une pression de 2 kb. On propose que la phase fluide représente un fluide magmatique résiduel extrait par une fracturation en profondeur.

[Traduit par le journal]

INTRODUCTION

The term 'high alumina alteration' was first used by Schmidt (1985) to describe the alteration assemblage: andalusite, diaspore, pyrophyllite, and topaz associated with gold deposits of the Carolina Slate Belt. He devised the term to distinguish the kaolinite and alunite types of hydrothermal alteration (i.e., advanced argillic) commonly seen in the upper part of some porphyry copper deposits from higher temperature equivalents containing andalusite.

High alumina hydrothermal alteration (HAHA) is associated with a variety of mineral deposit types. These deposit types include (i) porphyry type Cu – Mo$\pm$ Au deposits (Gustafson and Hunt, 1975; Brimhall, 1977; Steefel and Atkinson, 1984; and Schmidt, 1985); (ii) massive sulphide deposits (e.g., Boliden, Sweden, Nilsson, 1968; Chizevil, France, Lemiere et al., 1986); and (iii) epithermal Au$\pm$Ag deposits (e.g., Chetwynd, Nfld., McKenzie, 1986; Toodoggone, B.C., Panteleyev, 1986;

Carolina Slate Belt, USA, Schmidt, 1985). Although the mineral assemblage resulting from HAHA can vary, the presence of andalusite appears to be characteristic. The HAHA zone described in this paper is the first reported from the South Mountain Batholith (SMB) and is characterized by the hyperaluminous mineral assemblage, andalusite + sillimanite + cordierite + muscovite $\pm$ spinel, with accessory minerals including pyrite ($\leq$5%), fluorite, tourmaline, apatite, chalcopyrite, covellite, and rarely sphalerite.

The purpose of this paper is to describe and discuss various aspects regarding the petrography and mineral chemistry of the HAHA zone and host granitoid rocks. The nature of the hydrothermal system prevailing during the high alumina alteration will also be addressed.

GENERAL GEOLOGY

The HAHA zone is found within rocks of the Big Indian Polyphase Intrusive suite (BIPI suite,

Fig. 1). The BIPI suite is situated near the eastern margin of the SMB and is comprised of two large (18-20 km^2) granitoid bodies emplaced into a biotite granodiorite unit of the SMB (Corey, 1986; Ham and Horne, 1986). The SMB is a post-tectonic, peraluminous suite of granitoid rocks which occupies a large portion (10,000 km^2) of southwestern Nova Scotia. Details regarding its petrology, and geochemistry are well documented (McKenzie and Clarke, 1975; Clarke and Muecke, 1985; Clarke et al., 1985).

GEOLOGY OF THE BIPI SUITE

The BIPI suite has been divided into four mineralogically similar, but texturally variable units which include biotite ± muscovite and cordierite monzogranite, leucomonzogranite (≤6% biotite), leucogranite (≤2% biotite) and minor syenogranite (nomenclature after Streckeisen, 1976). The textural variations include: (1) medium-to-coarse grained to megacrystic; (2) porphyritic; (3) fine-to-medium grained; and (4) very fine-grained equigranular (herein termed microgranite). These units display sharp irregular contacts and contain abundant biotite granodiorite xenoliths (roof pendants?) which in turn possess numerous metasedimentary xenoliths of variable size (≤10 m^2) and shape. No metasedimentary xenoliths have been observed within rocks of the BIPI suite.

The unusual shape of the BIPI suite, together with zones of intense shearing both at contacts and internally suggests that its emplacement was controlled by pre-existing regional fault (basement?) structures. The occurrence of shear fabrics both within and adjacent to the BIPI suite may represent rejuvenation of some of these structures.

A well exposed series of NW trending, steeply dipping faults (and mylonite zones) which separate the BIPI suite into two halves suggests that at one time the BIPI suite constituted a single pluton.

PETROGRAPHY OF THE BIPI SUITE

The above units of the BIPI suite are characterized by containing variable amounts of the hyperaluminous mineral assemblage muscovite, garnet, cordierite, andalusite, and sillimanite.

Muscovite displays a variety of textures (all which imply subsolidus growth) and habits, ranging from large euhedral laths which have overgrown other minerals to fine-grained, anhedral crystals and crystal masses (sericite) which occur both surrounding and replacing other minerals (e.g., K-feldspar, plagioclase, biotite, garnet, aluminosilicate).

Aluminosilicates most commonly are small (≤1 mm) subhedral to anhedral andalusite crystal remnants hosted by and replaced (mantled) by muscovite (sericite) and also cordierite (pinite). Small (≤1 mm) euhedral crystals of andalusite were also observed within a sample of microgranite. Sillimanite (except in the HAHA zone) is restricted to fibrolitic masses within microfractures and surrounding garnets.

Cordierite, invariably pinitized, occurs both as anhedral crystals replacing andalusite and coexisting with it as small (≤1 mm) subhedral crystals within muscovite.
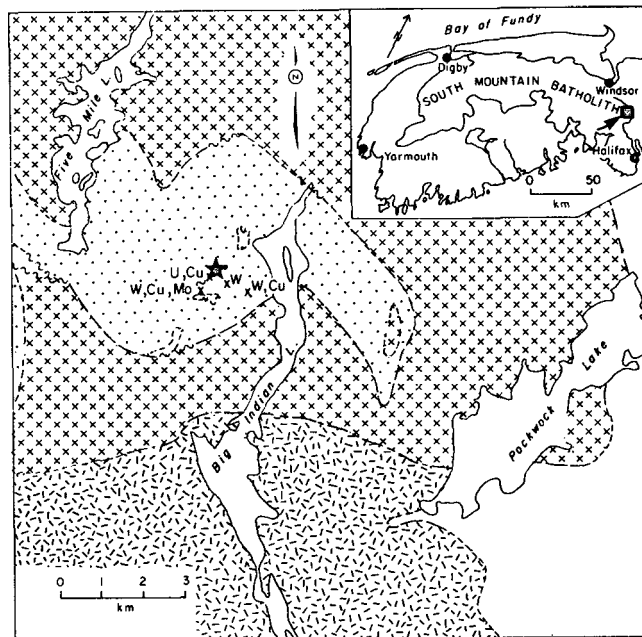
LEGEND

☐ undivided metasediments of the Meguma Group

biotite granodiorite

biotite ± muscovite ± cordierite monzogranite

undivided rocks of the Big Indian Polyphase Intrusion (see Table I)

Mineral occurrence .... x^W

Site of high alumina alteration pod .... ★

Shear zone .... ＶＶＶ

Fig. 1. General geology and location map for study area, showing HAHA zone and mineral occurrences.

Garnet commonly occurs as ≤1 cm anhedral polycrystalline (with quartz, sphene, and fibrolite) aggregates disseminated throughout the rocks and in narrow, K-feldspar-rich dykes which cross-cut the microgranite. Garnet is spessartine-rich and displays a strong antithetic relationship with biotite. A metasomatic origin has been suggested based on textural and chemical evidence (Kontak and Corey, in press).

ALTERATION AND MINERALIZATION

Figure 2 summarizes the various types and styles of alteration observed within the units of the BIPI suite. It is apparent from this figure that although metasomatic effects are present in all units, they are most intense within and proximal to the microgranite. This strongly suggests a genetic link between the fluids associated with the microgranite and the metasomatic-hydrothermal process.

Several different types of mineralization occur within the BIPI suite (Figs. 1, 2). Perhaps the most significant economically are the N-S trending, steeply dipping, enechelon quartz veins which contain coarse disseminations of wolframite (altering to scheelite), with minor chalcopyrite and molybdenite. The veins vary in width from 1 to

10 cm and are confined to the microgranite. The irregular shape and vuggy nature of the veins suggest that they filled dilatant zones within the microgranite.

Also located within the microgranite are chlorite, albite and tourmaline-bearing greisen veins and small (≤ 10 cm^2) pyrite- and chalcopyrite-bearing greisen pods. The greisen veins have the same orientation as the quartz veins and no cross-cutting relationships were observed.

Low-grade uranium-phosphate (torbernite $\pm$ autunite) and minor chalcopyrite mineralization associated with intense hematization is restricted to a prominent NE-trending shear zone which transects all phases of the BIPI suite.

The occurrence of tourmaline and fluorite are rare within the BIPI suite and appears to be associated with the later stages of hydrothermal activity. Evidence for this is the occurrence of several small (≤ 20 cm^2) pods of massive black tourmaline within a NE-trending shear zone.

Field observations (Fig. 2) suggest that repeated and superimposed periods of alteration and mineralization occurred within the BIPI suite and that early pervasive styles of alteration (pervasive garnet metasomatism) and mineralization (greisen pods) were overprinted by later, fracture-controlled styles (HAHA zone, W-bearing quartz veins).

Pollard and Taylor (1986) proposed that such a transformation is due to progressive fracturing in response to increasing fluid pressure accompanied by tapping of a magmatic fluid reservoir at different evolutionary stages. The presence of extensive microfracturing within the microgranite and prominent later shearing which cross-cut all BIPI suite units suggests that a process of progressive fracturing occurred.

HIGH ALUMINA HYDROTHERMAL ALTERATION ZONE

The HAHA zone forms a lenticular body approximately 10 m long x 3 m wide within the same shear zone that hosts the U-Cu mineralization. The occurrence of an intensely hematitized and autunite-bearing portion of the HAHA zone indicates that it was a product of an earlier metasomatic event which was overprinted by U-bearing fluids. In outcrop the HAHA zone is characterized by the presence of abundant ($\leq 20\%$) euhedral andalusite in addition to sillimanite, spinel, muscovite, disseminated pyrite ($\leq 5\%$), minor chalcopyrite, covellite, sphalerite, and light green apatite. Garnet and quartz are absent from the zone of HAHA, although both are present in rocks immediately surrounding it.

Mineralogy, Petrography and
   ## Mineral Chemistry of HAHA Zone

Table 1 provides a description of the principal mineral phases within the HAHA zone and summarizes the textures and phase relationships discussed below. Mineral chemistry data was collected using a Jeol 733 electron microprobe located at Dalhousie University, Nova Scotia. The microprobe utilizes four wavelength spectrometers with a Tracor Northern 145 ev Energy Dispersive System using the following operating parameters: accelerating
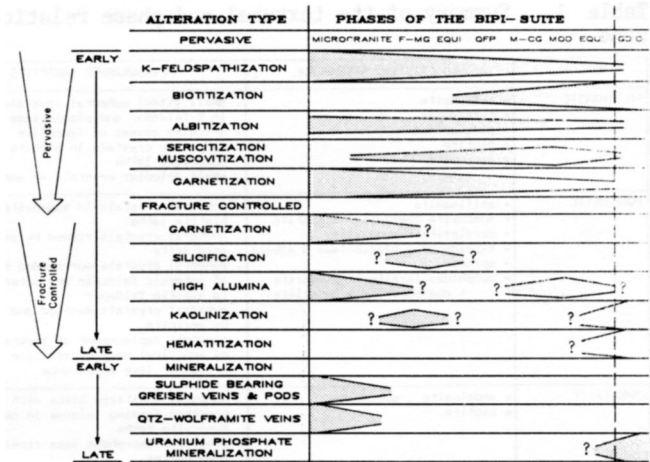

Fig. 2. Chronological sequence of alteration and mineralization types within the BIPI suite. Alteration exhibits transition in style from early pervasive to later fracture controlled. The unit in which the alteration is observed is also displayed; the units are listed beginning with the latest intrusive(?) unit (microgranite). The wider the bar the more intense the particular type of alteration.

voltage, 15 kV; probe current, 5 nA; counting time, 40 sec/element. A Tracor Northern ZAF MATRIX correction program was also used.

Andalusite

In hand sample andalusite is readily observed as long (≤ 2.5 cm), pinkish-red crystals commonly surrounded by a halo (≤ 3 mm) of light orange feldspar. In thin section the andalusite occurs as euhedral to subhedral crystals and crystal aggregates of prismatic to stubby habit (Plate 1a) overgrowing and replacing mineral phases, particularly plagioclase feldspar. Inclusions of albite, biotite, muscovite, and rare spinel and sillimanite were observed (Plate 1b). The andalusite commonly exhibit intense pleochroism (τ pink-mauve, α colourless) and a well developed muscovite (sericitic) alteration rim. Some andalusite has been completely pseudomorphed by sericite, whereas others only display sericitic replacement of crystal cores (donut texture). Irregular islands of andalusite, together with cordierite and rare K-feldspar, also occur within large ragged laths of muscovite.

Andalusite can also be associated with pyrite and other sulphides which occupy voids and fractures and partially envelope the crystals (Plate 1c).

Microprobe analyses (Table 2) indicate that andalusite is not a pure phase. The most abundant impurity is FeO_T, probably Fe^{3+} as it substitutes for Al^{3+} forming the complex $(FeAl)Si_2O_5$ (Grambling and Williams, 1985). The andalusite displays a strong Fe zonation (Fig. 3), with cores containing considerably more FeO_T than the rims (0.54-1.99 wt.% vs 0.41-0.61 wt.% FeO_T). Other impurities within the andalusite include CaO, K_2O, MgO, MnO and Na_2O. These impurities are present in very low concentrations and exhibit no zonation with the most abundant being MnO (≤ 0.11 wt.%) and Na_2O (≤ 0.07 wt.%).

Table 1. Summary of the textural and phase relationships of the principle mineral phases within the HAHA zone.

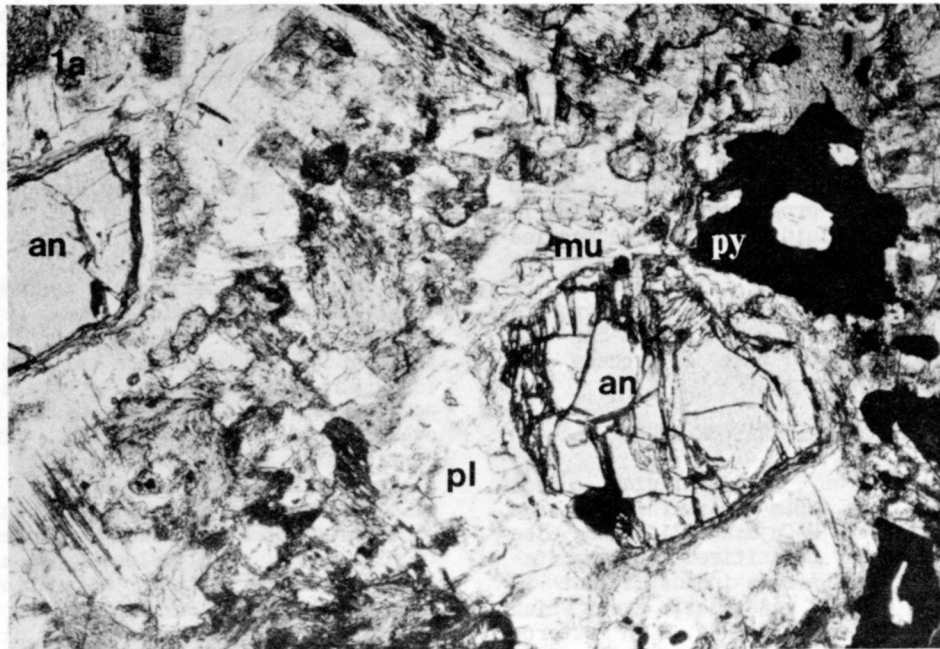| MINERAL	CO-EXISTING ASSEMBLAGE	PETROGRAPHIC VARIETIES	INCLUSIONS	ALTERATION
SILLIMANITE	+ andalusite + K-feldspar + plagioclase + biotite + muscovite	. small (<1mm) euhedral crystals in K-feldspar and plagioclase . acicular masses of fibrolite . fibrolite crystals in biotite and muscovite laths . small acicular crystals in andalusite	none	. polymorphic replacement by andalusite . pseudomorphic replacement of/by biotite and muscovite indicated by peculiar fibrous habit of micas
ANDALUSITE	+ sillimanite + muscovite (sericite) ± biotite + cordierite ± muscovite + k-feldspar + plagioclase ± albite + spinel + sulphides (pyrite ± sphalerite ± chalcopyrite + covellite)	. anhedral crystals in muscovite and biotite laths . anhedral crystals rimmed by pinitized cordierite . euhedral crystals surrounded by halo of potassic feldspar and intermediate to albitic feldspar . euhedral crystals mantled and replaced by sericite . complete replacement of crystal core by spherical mass of sericite creates a 'donut' like appearance	. sillimanite . spinel . biotite . muscovite (sericite) . albite	. sericite mantles surrounding crystals . partial to complete replacement of crystals by muscovite (sericite) . andalusite islands in large euhedral laths of secondary muscovite . pseudomorphic replacement by muscovite . partial to complete replacement of cyrstals by pinitized cordierite
CORDIERITE	+ andalusite ± muscovite + biotite	. anhedral pinitized blebs with andalusite together forming islands in secondary muscovite laths . pinitized amorphous mass rimming andalusites . pinitized crystals with biotite laths	none	. pinite
HERCYNITIC SPINEL	+ andalusite	. anhedral grains occuppying core of andalusite crystals	none	none

Plate 1a. Andalusite crystals surrounded by bleached halo composed of oligoclase (An_{11}–An_{16}). Clustered around the perimeter are masses of pinite and biotite. Field of view is 1 mm. an: andalusite, mu: muscovite, pl: plagioclase, py: pyrite.

Sillimanite

This mineral phase is most commonly observed as small (1-3 mm), euhedral crystal clusters and basal sections within laths of biotite and muscovite (Plate 1d). Sillimanite is more rarely seen as inclusions within plagioclase feldspar and andalusite.

Compared to andalusite, sillimanite contains less FeO_T (0.18-0.59 wt.%) but similar concentrations of CaO, Na_2O and K_2O (Table 2). No chemical zonation was observed.

Spinel

This mineral phase occupies the cores of andalusite crystals (Plate 1b) as dark emerald green anhedral crystals which have been identified as hercynite-rich spinel ($FeZnAl_2O_4$). The spinels are iron-rich (27.64-29.27 wt.% FeO_T), contain significant amounts of ZnO (10.9-12.38 wt.%), with minor MnO (0.85-1.01 wt.%) and MgO (0.55-0.69 wt.%) (Table 3).

Cordierite

Light to dark brown, amorphous, pinitized cordierite commonly mantles and pseudomorphs andalusite crystals. Cordierite also occurs with spherical masses of sericite which may represent completely altered andalusite. Small (<1 mm) intergrowths of pinitized cordierite and chloritized biotite also occur. The pinitized
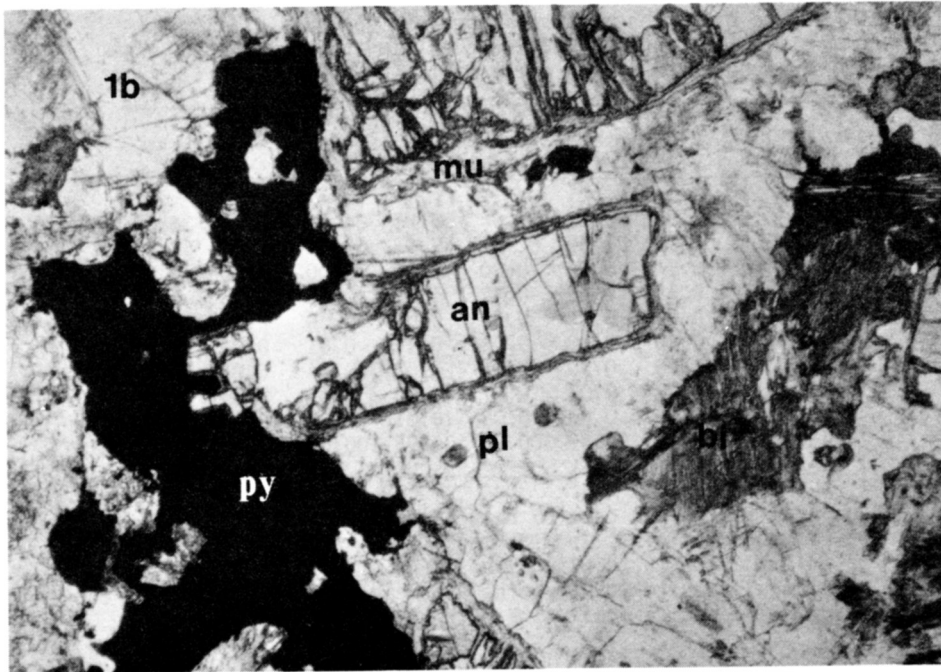
Plate 1b. Euhedral andalusite crystal exhibiting a sericitic alteration rim and feldspar halo is partially enveloped by late-stage pyrite (opaque). Field of view is 1 mm.
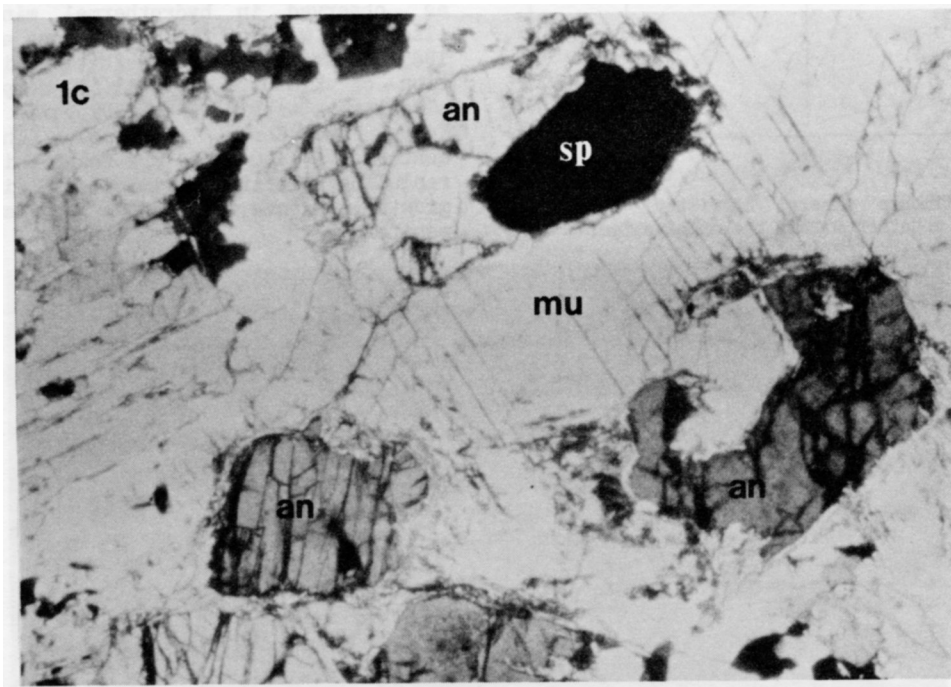

Plate 1c. Small (<1 mm) hercynite-spinel grain (isotropic) occupying core of andalusite crystal.   Field of view is 0.4 mm. sp: spinel

nature of the cordierite did not allow reliable microprobe analyses.

Muscovite

Muscovite observed within the HAHA zone is obviously secondary, and occurs as several textural types, including (1) sericitic mantles surrounding andalusite, (2) laths of muscovite containing andalusite and cordierite islands, (3) pseudomorphs of both sillimanite and andalusite, and (4) irregular laths replacing biotite and sillimanite (± fibrolite) intergrowths. The micas commonly display a peculiar fibrous habit which may indicate pseudomorphic replacement of sillimanite.

The white mica is essentially a pure end member

Table 2. Representative microprobe analyses of alumino-
silicates from the HAHA zone. A rim-core pair represent
analyses from a single crystal.

	1R	1C	2R	2C	3	4	5
SiO_2	32.32	36.88	36.94	36.85	36.28	36.38	36.64
Al_2O_3	62.09	61.39	62.74	62.92	63.31	63.49	62.86
TiO_2	0.07	0.02	0.00	0.00	0.00	0.00	0.00
FeO_T	0.55	1.18	0.42	1.01	0.31	0.53	0.38
MnO_T	0.00	0.04	0.00	0.00	0.00	0.00	0.00
MgO	0.00	0.06	0.02	0.11	0.01	0.01	0.01
CaO	0.00	0.00	0.04	0.02	0.04	0.03	0.06
Na_2O	0.04	0.02	0.07	0.05	0.05	0.00	0.06
K_2O	0.00	0.00	0.02	0.01	0.03	0.03	0.00
TOTAL	100.06	99.57	100.24	100.96	100.03	100.47	100.00

1,2: rim(R) and core(C) sets of andalusites; all occur
as euhedral cyrstals with muscovite mantles
4: sillimanite in oligoclase
5: sillimanite (overgrowths?) coexisting with biotite
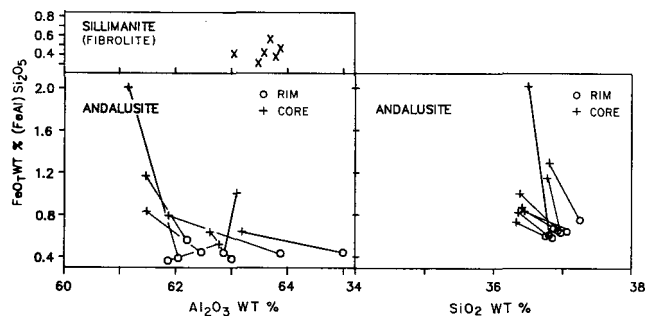6: sillimanite coexisting with oligoclase and biotite

Fig. 3. Aluminosilicate mineral chemistry; note the
strong $(FeAl)Si_2O_5$ zonation within the andalusites.

muscovite (Fig. 4, Table 4) with a minor amount cf
phengitic substitution (atomic prop. Si-3.02-3.16)
as observed in hydrothermal mineral deposits
elsewhere within the SMB (Strong and Chatterjee,
1985). Muscovite also exhibits a higher concentra-
tion of K_2O wt.% (10.9-11.5) compared to those
elsewhere within the BIPI suite (average 9.5;
Kontak and Corey, in press). The highest K_2O
contents ($\approx$11.0 wt.%) are found within muscovite
replacing biotite-sillimanite (± fibrolite) inter-
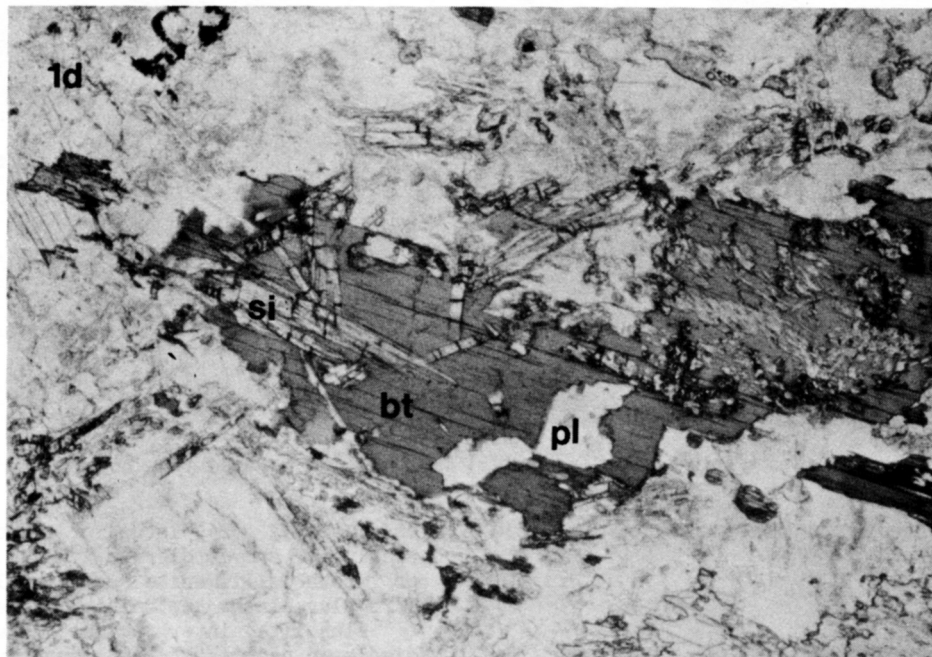growths and ones which appear to pseudomorph silli-
manite.

Plate 1d. Large flake of secondary biotite containing abundant sillimanite (fibrolite) crystals. Note that the
sillimanite is not confined to the biotite. Field of view is 0.4 mm. si: sillimanite, bi: biotite.

Table 3. Representative micro-
probe analyses of spinel from the
HAHA zone.

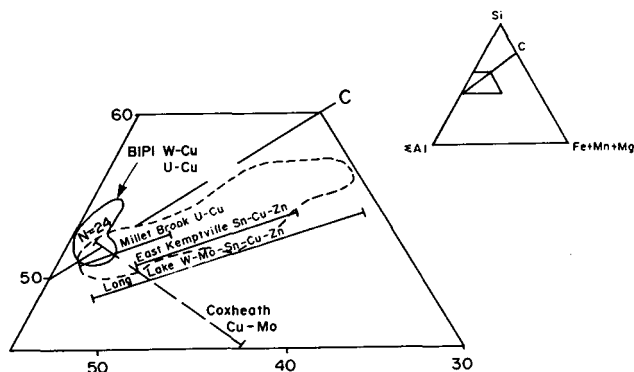|	1	2	3
Al_2O_3	57.53	57.98	57.09
FeO_T	27.64	27.84	29.27
ZnO	12.38	11.54	10.90
MnO	1.01	0.92	0.85
MgO	0.55	0.55	0.69
TiO_2	0.09	0.03	0.08
TOTAL	99.20	99.85	99.87

Fig. 4. Muscovite compositions from the HAHA zone plotted
in the ΣAl-Si-(Fe+Mn+MG) diagram (modified from Kontak
and Corey, in press). Analyses are compared to musco-
vites analyzed by Strong and Chatterjee (1985) from other
hydrothermal mineral deposits within Nova Scotia
(enclosed by heavy dashed line).

Biotite

This mineral is not an abundant phase within the
HAHA zone and commonly occurs as anhedral
chloritized flakes which exhibit varying degrees of
muscovite replacement. Anhedral, dark brown laths
were also observed coexisting with sillimanite and
intergrown with cordierite as small clots. Biotite
rarely occurs as an inclusion within andalusite.

With the exception of the HAHA zone analyses,
biotite shows a progressive enrichment in FeO_T and
Al_2O_3 wt.% and depletion in K_2O, Na_2O, TiO_2 and MgO
wt.% from granodiorite to microgranite (Fig. 5,
Table 5); MnO wt.% exhibits only a slight deple-
tion. Biotite from the HAHA zone deviates from the
above trends by being depleted in FeO_T and enriched
in MnO, MgO, K_2O, and Na_2O wt.% compared to biotite
from the microgranite phase of the BIPI suite. The
Al^{VI} versus Ti cationic plot for biotite (Fig. 6)
displays a trend of decreasing Ti (0.44-0.06) and
increasing Al^{VI} (0.42-1.36) from the granodiorite
to HAHA zone.

Biotite from the microgranite phase contain the
highest Fe/(Fe + Mg) ratios (0.87), with those from
the HAHA zone and biotite granodiorite xenoliths
containing lower ratios (0.8 and 0.62 respect-
fully; Fig. 7). Biotite from the microgranite and
HAHA zone has a higher ratio when compared to the
field for peraluminous granites (Clarke, 1981) but
are similar in their Fe enrichment compared to

other hydrothermal systems within the SMB (Strong
and Chatterjee, 1985).

Feldspars

Oligoclase is the most common plagioclase
observed within the HAHA zone and occurs as a halo
surrounding andalusite-muscovite intergrowths.
These haloes are of two types: (1) a optically
continuous crystal in which andalusite appears to
have replaced the plagioclase core, and (2) a
feldspar mosaic composed of several crystals. This
latter type, although comprised predominately of
oligoclase, may contain finely twinned albite.
Albite also occurs as inclusions within andalusite.
Minor orthoclase occurs as small blebs within
albite and oligoclase suggesting it is a product of
later K-feldspathization.

Figure 8 compares feldspar hosting andalusite
crystals within the zone of HAHA to the fields
defined by Kontak and Corey (in press) for feldspar
seen elsewhere within the BIPI suite. The majority
of feldspar from the HAHA zone is oligoclase
(An_{8-16}), although albitic (An_{0-9}) and potassic
(Or_{86-89}) feldspars are present (Table 6). It is
evident that a strong compositional similarity
exists between these feldspars and those from
monzogranite of the BIPI suite.

Apatite

Apatite is light-green in colour and ranges in
size from 2-5 mm. It overgrows all other minerals
phases and thus appears to have been the last
mineral to crystallize. A Pb-P mineral (pyromor-
phite?) was observed as a fracture filling within
the apatites. In Table 7 the composition of
secondary apatites from the HAHA zone and Phase 1
of the BIPI suite are presented and compared to
primary apatite occurring as inclusions within
biotite from granodiorite xenoliths. It is
apparent that while they all contain similar levels
of F, the secondary apatites are significantly
enriched in Mn, Cl, Fe and depleted in Ca.
Furthermore, the apatite from the HAHA zone
displays an enrichment in F and Fe and depletion in
Mn from core to rim.

DISCUSSION

Interpretation of Mineral Chemistry

Aluminosilicates

As mentioned above, the andalusite is
characterized by intense pleochroism reflecting a
strong iron (Fe^{3+}) zonation. Grambling and
Williams (1985), who studied aluminosilicates from
Precambrian metamorphic rocks of northern New
Mexico, suggest that the ability of andalusite to
absorb iron is a function of pressure, temperature
and oxygen fugacity; a decrease in pressure and/or
increase in temperature and oxygen fugacity permits
greater Fe^{3+} uptake. The strong Fe enrichment
within the cores of andalusites in the HAHA zone
would imply that these parameters changed
during crystallization of andalusite. Previous
studies of andalusite from the SMB (Clarke et al.,
1976) and its thermal metamorphic aureole
(Jamieson, 1974) indicated some Fe^{3+} substitution

Table 4. Representative microprobe analyses of muscovite from
the HAHA zone. Structural formulae based on 22 O.

	1	2	3	4	5	6	7	8
SiO_2	46.26	46.00	46.12	45.68	44.86	45.75	48.19	46.34
Al_2O_3	35.84	36.48	36.59	35.31	36.89	35.36	35.34	35.94
TiO_2	0.00	0.00	0.00	0.07	0.02	0.28	0.02	0.08
FeO_T	1.22	1.08	1.56	1.75	0.84	1.51	1.60	1.14
MnO	0.06	0.06	0.05	0.00	0.01	0.11	0.06	0.00
MgO	0.34	0.22	0.29	0.46	0.12	0.37	0.20	0.30
CaO	0.02	0.00	0.00	0.00	0.02	0.03	0.00	0.03
Na_2O	0.46	0.41	0.89	0.86	0.40	0.66	0.46	0.58
K_2O	11.27	11.53	10.91	10.94	11.19	10.37	10.24	11.07
TOTAL	95.45	95.78	96.41	95.07	94.35	94.44	96.11	95.48
Si_{iv}	6.163	6.113	6.092	6.133	6.039	6.151	6.327	6.163
Al_{iv}	1.837	1.887	1.908	1.867	1.961	1.849	1.673	1.837
Al^{vi}	3.790	3.826	3.788	3.719	3.891	3.752	3.794	3.796
Ti	0.000	0.000	0.000	0.007	0.002	0.028	0.002	0.008
Fe	0.136	0.120	0.172	0.196	0.095	0.170	0.176	0.127
Mn	0.007	0.007	0.006	0.000	0.001	0.013	0.007	0.000
Mg	0.068	0.044	0.057	0.092	0.024	0.074	0.039	0.059
Ca	0.003	0.000	0.000	0.000	0.003	0.004	0.000	0.004
Na	0.119	0.106	0.288	0.224	0.104	0.172	0.117	0.150
K	1.915	1.954	1.838	1.873	1.921	1.778	1.715	1.878

fibrous muscovite (pseudomorphing sillimanite ?): 1,2
secondary lath containing sillimanite: 8
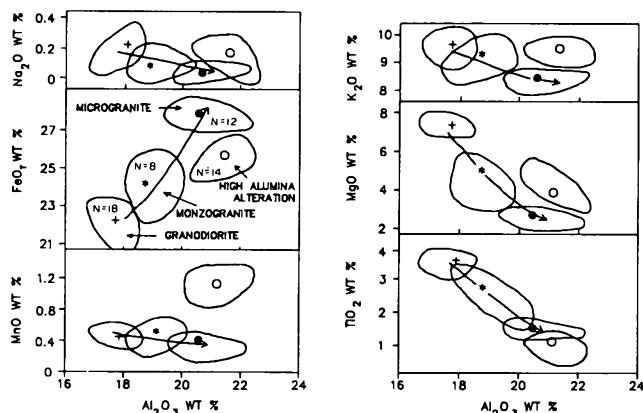secondary lath containg andalusite + cordierite: 5,6
mantle around andalusite: 3,4,7

Fig. 5. Oxide wt.% contents of biotites from units of the
BIPI suite versus their Al_2O_3 wt.%. Symbol location
represents average analyses for units, whereas variation
within each unit is denoted by circle surrounding symbol.
Arrows represent assumed magmatic/metasomatic trends.

with FeO_T concentrations of 0.45 ± 0.17 wt.% and
0.81 ± 0.83 wt.%, respectively. Although no zona-
tion was reported, Clarke et al. (1976) indicated
that some andalusite exhibited colourless to pink
pleochroism, which may (as observed in this study)
reflect Fe^{3+} zoning.

Although andalusite is the most abundant phase,
the presence of the mineral assemblages
sillimanite-oligoclase, sillimanite-andalusite, and
sillimanite-biotite indicate that the fluids
attending metasomatism were initially above the
andalusite stability field (620°C @ 2 kb; Robie and

Hemingway, 1984). Equilibration with lower
temperature fluids is indicated by the presence of
abundant secondary muscovite surrounding and
replacing andalusite.

Spinel

The presence of spinel (hercynite inclusions in
andalusite) within the HAHA zone implies an
environment characterized by high temperature, low
silica activity and high oxygen fugacity (Clarke,
1981). The only previous documented occurrence of
spinel within the SMB was by Farley (1979), who
mentioned the presence of ≤5 mm cubes and
disseminations of gahnite-rich spinel (25.32 wt.%
ZnO; 18.74 wt.% FeO_T) within a greisenized
pegmatite and aplite. Spry (1987), in describing
compositional zonation in gahnite spinels
worldwide, indicated that hercynite is stabilized
to lower temperatures (<750°C) by Zn in the
presence of quartz.

Muscovite

Experimental studies by Monier and Robert (1986)
have determined that increasing phengitic and
biotitic substitution in muscovite reflects
decreasing crystallization temperatures. Compari-
son of the BIPI suite data to the Monier and Robert
(1986) cation diagram (Fig. 9) indicates that
hydrothermal muscovite within the HAHA zone and
BIPI suite granitoids crystallized at high tempera-
tures (≥500°C at 2 kb; Monier and Robert, 1986).
This is consistent with the presence of the mineral

Table 5. Representative microprobe analyses of biotite from the BIPI suite and HAHA zone. Structural formulae based on 22 O.

	21	22	23	24	25	26	27	28
SiO_2	34.35	34.28	34.24	34.35	33.65	34.51	35.66	34.35
Al_2O_3	21.16	21.36	21.78	21.33	21.73	22.30	20.40	21.05
TiO_2	1.16	0.93	0.56	0.58	1.56	1.01	1.79	1.18
FeO_T	25.58	25.56	25.25	25.62	26.26	25.22	22.40	25.18
MnO	1.18	1.05	1.08	1.29	0.45	1.29	0.95	0.90
MgO	3.65	3.69	3.77	3.84	3.20	3.11	5.56	3.65
CaO	0.00	0.05	0.00	0.02	0.00	0.00	0.00	0.02
Na_2O	0.06	0.06	0.21	0.28	0.28	0.01	0.22	0.21
K_2O	9.43	9.84	9.02	9.44	9.61	9.44	9.50	9.29
TOTAL	96.56	96.82	95.89	96.75	96.73	96.87	96.47	95.83
Si	5.331	5.315	5.326	5.328	5.229	5.316	5.441	5.355
Al_{iv}	2.669	2.685	2.674	2.672	2.771	2.684	2.559	2.645
Al^{vi}	1.200	1.218	1.318	1.226	1.207	1.364	1.109	1.223
Ti^{vi}	0.135	0.108	0.066	0.068	0.182	0.117	0.205	0.138
Fe	3.320	3.314	3.284	3.323	3.412	3.249	2.858	3.283
Mn	0.155	0.138	0.142	0.169	0.059	0.168	0.123	0.119
Mg	0.844	0.853	0.874	0.888	0.741	0.714	1.264	0.848
Ca	0.000	0.008	0.000	0.003	0.000	0.000	0.000	0.003
Na	0.018	0.018	0.063	0.084	0.084	0.003	0.065	0.063
K	1.867	1.946	1.789	1.867	1.905	1.855	1.849	1.847
Fe/Fe+Mg	0.797	0.795	0.790	0.789	0.821	0.819	0.694	0.794

22,23,26: coexist with sillimanite and plagioclase
21: contains andalusite
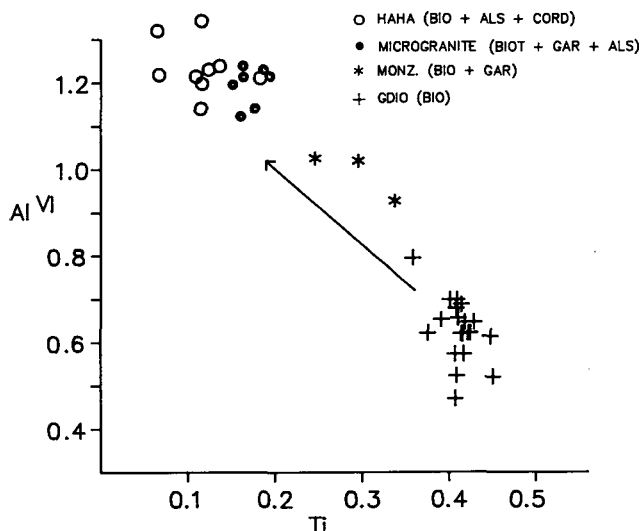25,27: are inclusions within andalusite
24,29: seperate grains

Fig. 6. Al^{vi} versus Ti plot (adapted from LeBel, 1979), for biotites from the BIPI suite. Arrow shows decreasing temperature of biotite crystallization.

assemblage muscovite-andalusite-albite which, according to thermodynamic studies by Helgeson (1985), indicates a temperature of <600°C at 2 kb.

Biotite
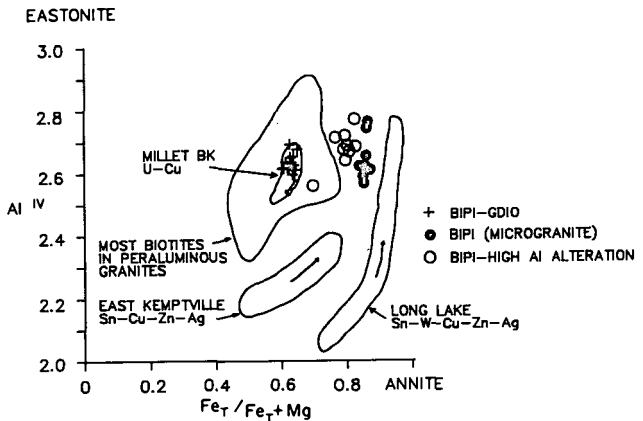
A trend of decreasing Ti has been reported by a

Fig. 7. Al^{iv} over Fe/(Fe+Mg) plot for biotites from the BIPI suite. Comparisons are made to Clarke's (1981) field for biotites in peraluminous granites and also those defined by Strong and Chatterjee (1985) for biotites from other hydrothermal mineral deposits within the SMB.

number of authors for hydrothermal biotites from several porphyry copper deposits (e.g., Le Bel, 1979; Jacobs and Perry, 1979; Bowman et al., 1987). Similarly, a study by Dilles (1987) of biotite within alteration zones associated with porphyry copper mineralization within the Yerington Batholith suggests that an increase in Ti reflects an increase in equilibration temperature. Thus the
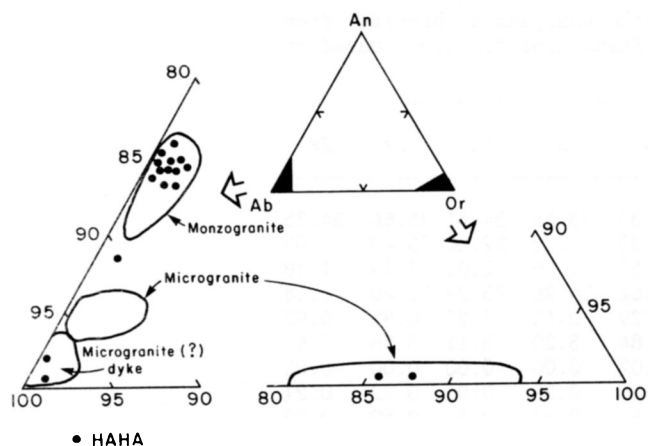
• HAHA

Fig. 8. Composition of feldspars from the HAHA zone (solid dots) plotted in the An–Ab–Or diagram. Data is compared to fields delineated by Kontak and Corey (in press) for several units of the BIPI suite.

lower contents for biotite from the HAHA zone suggests that these micas equilibrated at lower temperatures than biotites in the units of the BIPI suite.

The lower $Fe/(Fe+Mg)$ ratio in biotite from the HAHA zone compared to biotite from the microgranite can probably be attributed to a combination of fluid chemistry, lower temperature, and higher oxygen fugacity. The latter would account for the Mg-enrichment in biotite from the HAHA zone.

Feldspars

The feldspar haloes surrounding andalusite-muscovite intergrowths within the zone of HAHA are either secondary, resulting from interaction of the granitic rock with a fluid phase, or represent remnant feldspars which were present within the leucomonzogranite prior to the high alumina metasomatism. The fact that andalusite appears to have crystallized within the cores of many plagioclase phenocrysts suggests the latter. Similar feldspar alteration has been widely accepted as being produced by intense hydrolysis attributed to interaction with a high temperature, silica-rich, acidic fluid. Assuming Al was inert, this process involved intense base leaching (removal of alkalis) with the crystallization of andalusite and perhaps even corundum at the appropriate temperature (Hemley *et al.*, 1980; Beane, 1982).

The pristine nature of the albite and the common occurrence of an albite-andalusite assemblage indicates that albite was stable during andalusite formation (≈ 600°C @ 2 kb) and perhaps may even have been a co-product of the reaction forming andalusite. These observations together with the relative absence of K-feldspar implies that either the metasomatising fluid was Na-rich, or, conversely, the physiochemical conditions attending the alteration event favoured the development of albite (e.g., high temperatures).

Nature of the Hydrothermal System

The replacement of oligoclase by aluminosilicates (± spinel), requires a significant amount of Al,

and would release Si, K, Na and Ca to the fluid assuming a constant volume reaction (as suggested by unpublished data). Although the late appearance of apatite would account for redeposition of the Ca, muscovite for K, and albite for Na, the fate of the silica is more problematic since the HAHA zone contains no free quartz. This differs from silica-rich, quartz-andalusite-pyrophyllite-bearing high-alumina zones commonly described in the literature. The absence of a vuggy texture which characterizes desilicified granitic rocks (Cathelineau, 1986) indicates that quartz removal within the HAHA zone was not a later event and suggests that the desilicification process occurred either before or in conjuction with the high alumina metasomatism. The absence of any secondary quartz and the early presence of spinel suggests that the fluid involved in the HAHA process remained silica-undersaturated.

Whether alumina was a component of the fluid and therefore a mobile element has not been ascertained by this study. However, the presence of fluid-derived alumina during development of the HAHA zone cannot be precluded. According to experimental studies by Anderson and Burnham (1983) to account for the appearance of feldspathoid by the dissolution of feldspar at high temperatures, Al can be transported in a fluid phase as an alkali complex. This process is temperature dependant (i.e., Al/Na ratio increases with temperature) and requires that the fluid be silica(H_4SiO_4)-poor and have a high Na-KCl/HCl ratio. This implies that Al complexing and transport is more significant where feldspars instead of micas are stable. These findings suggest that the ability of the silica-poor (±Na-rich) fluid (which attended the high alumina metasomatism) to transport Al was perhaps substantial. The occurrence of andalusite assemblages instead of feldspathoid indicates that a limited source of silica was available during metasomatism. However, the presence of spinel indicates that domains of low silica concentration did exist during the early stages of the alteration. Alternatively, if albite was co-precipitated with andalusite then silica may have also been consummed according to the reaction: oligoclase + Na(±Al)-fluid >> andalusite + albite + Ca.

The strong zonation of Fe within the andalusites marks a change in the iron species from ferric to ferrous. This, together with the low $Fe/(Fe+Mg)$ ratio of biotites in the HAHA zone, and the initial crystallization of hercynitic spinel, further implies that the fluid had a higher oxygen fugacity than that which affected the microgranite during earlier (auto?) metasomatism. Whether the increased oxygen fugacity is due to the presence of meteoric fluids or some other process (e.g., release of H_2 gas, formation of H_2S) remains unsolved and further studies will address this problem. Although the desilicified nature of the HAHA zone is suggestive of meteoric waters (Hemley *et al.*, 1980; Cathelineau, 1986), alternative processes are possible (e.g., quartz depletion in response albite formation). The presence of a Na(±Al)-rich, silica-poor residual magmatic fluid suggests that the bulk composition of the melt changed, a process perhaps related to the occurrence of earlier albitized and K-feldspathized rocks (Clarke and Muecke, 1985).

The chemistry of apatite indicates the existence

Table 6. Representative microprobe analyses of feldspar from the HAHA zone. Structural formulae based on 32 O.

	31	35	49	51	52	53	54	56
SiO_2	67.99	64.39	64.67	63.76	67.46	65.05	64.27	62.87
Al_2O_3	18.81	22.98	22.49	20.94	19.44	22.39	20.81	20.80
FeO_T	0.05	0.01	0.03	0.04	0.11	0.13	0.13	0.00
MgO	0.03	0.00	0.02	0.03	0.01	0.07	0.02	0.02
CaO	0.06	2.94	2.51	3.02	0.46	2.32	2.71	1.88
Na_2O	0.92	8.81	8.79	10.19	10.96	8.70	9.06	10.50
K_2O	10.09	0.28	0.29	0.26	0.16	0.46	0.32	0.22
TOTAL	97.95	99.41	98.80	98.24	98.60	99.12	97.32	96.29
Si	12.311	11.366	11.461	11.469	11.952	11.493	11.596	11.504
Al	4.014	4.780	4.697	4.438	4.058	4.662	4.424	4.485
Fe	0.008	0.001	0.004	0.006	0.016	0.019	0.020	0.000
Mg	0.008	0.000	0.005	0.008	0.003	0.018	0.005	0.005
Ca	0.012	0.556	0.477	0.582	0.087	0.493	0.524	0.369
Na	0.323	3.015	3.020	3.554	3.765	2.980	3.169	3.725
K	2.330	0.063	0.066	0.060	0.036	0.104	0.074	0.051
Or	87.44	1.73	1.84	1.42	0.93	2.94	1.95	1.23
An	0.44	15.30	13.37	13.87	2.24	12.46	13.91	8.89
Ab	12.12	82.96	84.78	84.70	96.82	84.59	84.13	89.86

inclusion in andalusite: 52
part of halo surrounding andalusite: 51,53,54,56
hosts sillimanite: 35,49
replacement of albite: 31

Table 7. Representative microprobe analyses of apatite from the HAHA zone.

	1R	1C	2R	2C	3	4	5	6
P_2O_5	40.16	41.02	39.61	40.68	40.24	40.26	41.62	41.12
CaO	50.56	51.03	50.61	51.76	50.99	49.10	54.78	54.33
MnO	2.43	3.45	2.51	2.55	3.37	3.75	0.81	0.73
MgO	0.06	0.00	0.06	0.02	0.12	0.11	0.04	0.00
FeO_T	1.11	0.53	0.98	0.81	1.07	1.18	0.33	0.36
Y_2O_3	0.14	0.26	0.10	0.07	0.00	0.08	0.20	0.31
SrO	0.03	0.01	0.00	0.02	0.00	0.00	0.00	0.04
F	3.34	1.75	3.12	2.47	2.59	3.28	1.90	2.81
Cl	0.15	0.14	0.12	0.14	0.36	0.44	0.11	0.08
TOTAL	97.98	98.20	97.11	98.49	98.74	98.20	99.79	99.78

1,2: rim(R) and core(C) sets from secondary apatites; HAHA zone
3,4: secondary apatites from altered leucomonzogranite (ph-1)
5,6: primary apatites as inclusions in biotite within grano-diorite

of a volatile-(F and P) and Mn-rich fluid phase during the late stages of hydrothermal activity. However, the presence of pyromorphite in fractures within the apatite and the subsequent overprinting of the HAHA zone by uranium-phosphate mineralization associated with intense hematization indicates that the waning stages of hydrothermal activity were also dominated by oxidizing fluids. The noted absence of garnets within the HAHA zone, although ubiquitous in the surrounding rocks, implies that the garnets were in disequilibrium with the fluid phase and may have possibly contributed to the Mn-rich nature of the fluid.

CONCLUSIONS

Phase assemblages and mineral chemistry suggest that the HAHA zone resulted by the interaction of a high temperature ($\geq 620^{\circ}$C @ 2 kb), Na($\pm$Al)-rich, silica-undersaturated fluid with rock of
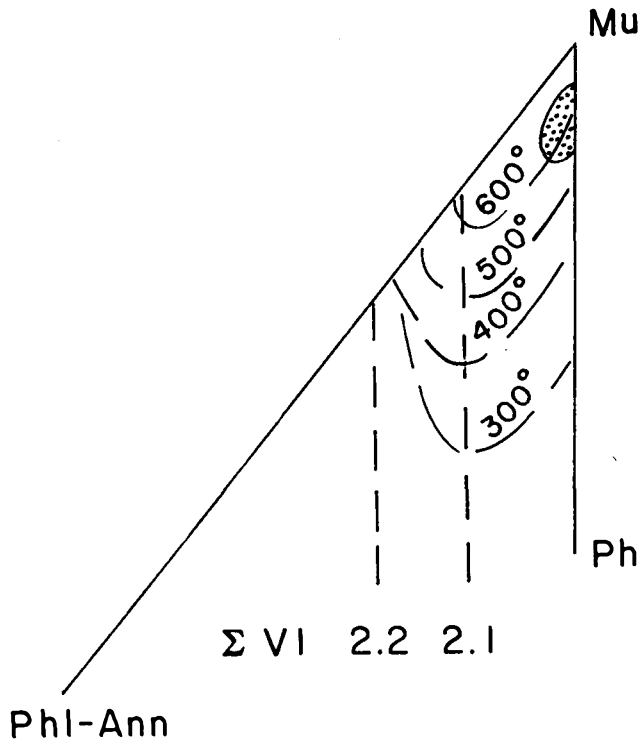
Mu

600°
500°
400°
300°

Ph

Σ Vl   2.2   2.l

Phl-Ann

Fig. 9. Muscovites of the HAHA zone (shaded area) plotted on the Σvi versus Si cation diagram of Monier and Robert (1986). Isotherms are shown by dashed (long) lines.

leucomonzogranite (unit 1) composition.

It is proposed that the fluid was of magmatic-hydrothermal origin, and that the fluid-reservoir was accessed by deep-seated faulting in response to increasing fluid pressure. The presence of numerous granodiorite xenoliths (roof pendants?) containing abundant Meguma Group metasedimentary xenoliths suggests that the evolution of the BIPI suite occurred at a relatively shallow level. The mineral chemistry of the various mineral phases within the HAHA zone and the nature of later superimposed alteration (hematitization) indicates that the magmatic-hydrothermal fluid possessed a high oxygen fugacity possibly reflecting interaction with meteoric fluids.

The occurrence of high alumina metasomatism within the SMB has implications beyond its association with a variety of mineral deposits. It represents but one of a series of superimposed metasomatic events which affected the BIPI suite and provides additional insight into interpreting the myriad of processes which operated within the SMB.

ACKNOWLEDGEMENTS

ANDERSON, G.M., and BURNHAM, C.W. 1983. Feldspar solubility and the transport of aluminum under metamorphic conditions. American Journal of Science, 283A, pp. 283-297.

BEANE, R.E. 1982. Hydrothermal alteration in silicate rocks, southwestern North America. In Advances in geology of the porphyry copper deposits, southwestern North America. Edited by S.R. Titley. The University of Arizona Press, Tuscon, Arizona, pp. 117-137.

BOWMAN, J.R., PARRY, W.T., KROPP, W.P., and KRUER, S.A. 1987. Chemical and isotopic evolution of hydrothermal solutions at Bingham, Utah. Economic Geology, 82, pp. 395-428.

BRIMHALL, G.H. JR. 1977. Early fracture-controlled disseminated mineralization at Butte, Montana. Economic Geology, 72, pp. 37-59.

CATHELINEAU, M. 1986. The hydrothermal alkali metasomatism effects on granitic rocks; quartz dissolution and related subsolidus changes. Journal of Petrology, 27, pp. 945-965.

CLARKE, D.B. 1981. The mineralogy of peraluminous granites: a review. Canadian Mineralogist, 19, pp. 3-17.

CLARKE, D.B., and MUECKE, G.K. 1985. Review of the petrochemistry and origin of the South Mountain Batholith and associated plutons, Nova Scotia, Canada. In High Heat Production (HHP) Granites, Hydrothermal Circulation and Ore Genesis. Institute of Mining and Metallurgy, London, England, pp. 41-54.

CLARKE, D.B., MUECKE, G.K., and CHATTERJEE, A.K. 1985. The South Mountain Batholith: Geology, petrology, geochemistry. In Guide to the Granites and Mineral Deposits of Southwestern Nova Scotia. Edited by A.K. Chatterjee and D.B. Clarke. Nova Scotia Department of Mines and Energy, Paper 85-3, pp. 1-15

CLARKE, D.B., MCKENZIE, C.B., MUECKE, G.K., and RICHARDSON, S.W. 1976. Magmatic andalusite from the South Mountain Batholith, Nova Scotia. Contributions to Mineralogy and Petrology, 56, pp. 279-287.

COREY, M.C. 1986. Bedrock geology of the South Mountain Batholith; NTS map sheet 11D/13. In Mines and Minerals Branch, Report of Activities, 1985. Edited by J.L. Bates. Nova Scotia Department of Mines and Energy, Report 86-1, pp. 137-148.

DILLES, J.H. 1987. Petrology of the Yerington Batholith, Nevada; evidence for evolution of porphyry copper ore fluids. Economic Geology, 82, pp. 1750-1787.

FARLEY, E.J. 1978. Mineralization of the Turner and Walker deposits of the South Mountain Batholith. Unpublished M.Sc. thesis, Dalhousie University, Halifax, Nova Scotia.

GRAMBLING, J.A., and WILLIAMS, M.L. 1985. The effects of Fe^{3+} and Mn^{3+} on aluminum siliciate phase relationships in north central New Mexico, USA. Journal of Petrology, 26, pp. 324-354.

GUSTAFSON, L.B., and HUNT, J.P. 1975. The porphyry copper deposit at El Salvador, Chile. Economic Geology, 70, pp. 857-912.

HAM, L.J., and HORNE, R.J. 1986. Geology of the South Mountain Batholith on the eastern half of NTS map sheet 21A/16. In Mines and Minerals Branch Report of Activities, 1985. Edited by J.L. Bates. Nova Scotia Department of Mines and Energy, Report 86-1, pp. 149-159.

HELGESON, H.C. 1985. Some thermodynamic aspects of geochemistry. Pure and Applied Chemistry, 57, pp. 31-44.

HEMLEY, J.J., MONTOYA, J.W., MARINENKO, J.W., and LUCE, R.W. 1980. Equilibria in the system Al_2O_3-SiO_2-H_2O and some general implications for alteration/mineralization processes. Economic Geology, 75, pp. 210-228.

JACOBS, D.C., and PARRY, W.T. 1979. Geochemistry of biotite in the Santa Rita porphyry copper deposit, New Mexico. Economic Geology, 74, pp. 860-887.

JAMIESON, R.A. 1974. The Contact of the South Mountain Batholith near Mount Uniacke, Nova Scotia. Unpublished B.Sc. thesis, Dalhousie University, Halifax, Nova Scotia.

KONTAK, D.J., and COREY, M.C. In press. Metasomatic origin for spessartine-rich garnets in the South Mountain Batholith, Nova Scotia. Canadian Mineralogist, 26.

LEBEL, L. 1979. Micas magmatiques et hydrothermaux dans l'environnement du porphyre cuprifere de Cerro Verde-Santa Rosa, Perou. Bulletin de Mineralogy, 102, pp. 35-41.

LEMIERE, B., DELFOUR, J., MOINE, B., PIBOULE, M., PLOQUIN, A., ISNARD, P., and TEGYEY, M. 1986. Hydrothermal alteration and the formation of aluminous haloes around sulfide deposits. Mineralium Deposita, 21, pp. 147-155

MACDONALD, M.A., and CLARKE, D.B. 1985. The petrology, geochemistry, and economic potential of the Musquodoboit Batholith, Nova Scotia. Canadian Journal of Earth Sciences, 22, pp. 1633-1642.

MCKENZIE, C.B. 1986. Geology and mineralization of the Chetwynd deposit, Southwestern Newfoundland, Canada. *In* Proceedings of Gold '86, An International Symposium on the Geology of Gold. *Edited by* A.J. MacDonald. Toronto, 1986, pp. 137-148.

MCKENZIE, C.B., and CLARKE, D.B. 1975. Petrology of the South Mountain Batholith, Nova Scotia. Canadian Journal of Earth Sciences, 12, pp. 1209-1218.

MILLER, C.F., STODDARD, E.F., BRADFISH, L.J., and DOLLASE, W.A. 1981. Composition of plutonic muscovite: genetic implications. Canadian Mineralogist, 19, pp. 25-34.

MONIER, G., and ROBERT, J.L. 1986. Muscovite solid solutions in the system K_2O-MgO-FeO-Al_2O_3-SiO_2-H_2O: an experimental study at 2 kbar PH_2O and comparison with natural Li-free white micas. Mineralogical Magazine, 50, pp. 257-266.

NILSSON, C.A. 1968. Wall rock alteration at the Boliden deposit, Sweden. Economic Geology, 63, pp. 472-494.

PANTELEYEV, A. 1986. Canadian Cordilleran model for epithermal gold-silver deposits. Geoscience Canada, 13, pp. 101-111.

POLLARD, P.J., and TAYLOR R.G. 1986. Progressive evolution of alteration and tin mineralization; controls by intersititial permeability and fracture-related tapping of magmatic fluid reservoirs in tin granites. Economic Geology, 81, pp. 1795-1800.

ROBIE, R.A., and HEMINGWAY, B.S. 1984. Entropics of kyanite, andalusite, and sillimanite: additional constraints on the pressure and temperature of the Al_2SiO_5 triple point. American Mineralogist, 69, pp. 298-306.

SCHMIDT, R.G. 1985. High alumina hydrothermal systems in volcanic rocks and their significance to mineral prospecting in the Carolina Slate Belt. United States Geological Society Survey Bulletin 1562.

STEEFEL, C.I., and ATKINSON, W.W., JR. 1984. Hydrothermal andalusite and corundum in the Elkhorn District, Montana. Economic Geology, 79, pp. 573-579.

STRONG, D.F., and CHATTERJEE, A.K. 1985. A review of some chemical and mineralogical characteristics of granitoid rocks hosting Sn, W, U, Mo deposits in Newfoundland and Nova Scotia. *In* High Heat Production (HHP) Granites, Hydrothermal Circulation and Ore Genesis. Institute of Mining and Metallurgy, London, England, pp. 489-516.

SPRY, P.G. 1987. Compositional zoning in zincian spinel. Canadian Mineralogist, 25, pp. 97-104.